Modeling of impact cratering in granular media

L.S. Tsimring & D. Volfson
Institute for Nonlinear Science, University of California, San Diego, La Jolla, CA 92093-0402

We simulate penetration of large projectiles into dry granular media using two-dimensional soft particle molecular dynamics. We systematically vary the physical parameters of the projectile (density, size, impact energy). Our results confirm the recently observed scaling of the crater depth with impact energy as observed by Uehara et al. (2003) and the effect of constant deceleration of the ball during the penetration phase as observed by Ciamarra et al (2004). We calculate the distribution of energy dissipation during the impact among different dissipation mechanisms and conclude that most dissipation occurs due to internal frictional contacts among the grains. We also propose a model which describes the observed scaling regimes of impact cratering.

1 INTRODUCTION

Study of impact cratering has a long and rich history starting from the pioneering works by Robins, Euler, Poncelet and others (Robins 1742; Euler 1745; Poncelet 1829). Most of this work, motivated by military or geophysical applications, was concerned with high-speed impacts when the body penetrates deep into the medium.

The renewed interest in this problem has emerged recently in granular physics (Uehara et al. 2003; Newhall & Durian 2003; Walsh et al. 2003; de Bruyn & Walsh 2004; Ciamarra et al. 2004), with an emphasis on relatively low-speed impact cratering. Uehara et al. (Uehara et al. 2003) found a non-trivial scaling of the crater depth with the total energy of the penetrating body in the case of low-speed impact. Ciamarra et al. (Ciamarra et al. 2004) studied the penetration of a circular disk in a two-dimensional system and found that during a prolonged "penetration phase" the deceleration of the disk is roughly constant and proportional to the initial impact velocity. They also performed soft particle molecular dynamics simulations of an analogous system and found similar behavior.

In this work we present the results of our 2D molecular dynamics simulations of the low-speed impact cratering in dry granular media. We focus our attention on the energetic aspects of cratering, specifically, on the main channels and mechanisms of energy dissipation during impact. In addition, we address the issue of penetration depth scaling which has caused some controversy in recent literature.

2 MOLECULAR DYNAMICS SIMULATIONS

Impact cratering was simulated using two-dimensional soft particle molecular dynamics algorithm. Both projectile and grains were modeled as non-cohesive, dry, inelastic, disk-like particles. Two grains interact via normal and shear forces whenever they overlap. For the normal impact we employed *spring-dashpot* model (Schäfer et al. 1996), and the Cundall-Strack model for tangential forces (Cundall & Strack 1979). The granular bed was prepared by dropping 20,000 particles into a rectangular container 100×200 particle diameters and compacting them by shearing and taping with a rough upper wall (which was subsequently removed). We employed periodic boundary conditions in the horizontal direction, and used fixed particles at the bottom of the container. The material parameters of grains were chosen similar to (Volfson et al. 2003). To avoid crystallization we introduced slight polydispersity of the grains. All quantities are normalized by an appropriate combination of the average grain diameter d_g, mass m_g, and gravity g. The mean density of granular bed after preparation ρ_g was close to the random close packing density 0.82.

In a typical simulation, a ball (two-dimensional disk) of diameter D_b and density ρ_b touching the horizontal free surface of the granular bed was released with downward initial velocity v_0. Figure 1 shows two snapshots corresponding to the early and late phases of the low-speed impact. In order to study the resistance forces in granular media during impact and the mechanisms of energy dissipation we systematically varied the projectile size, density, and impact velocity, as well as friction among the grains. There are several alternative channels of energy redistribution

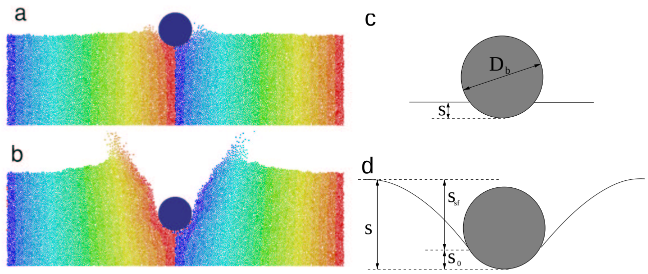

Figure 1: a,b - two snapshots from a single run with $D_b = 30, \rho_b/\rho_g = 2, \mu = 0.3, v_0 = 13.85$ corresponding to the initial phase and late phase of the ball penetration; c,d - sketches of these two phases. Shades of gray n a,b indicate the initial horizontal position of grains

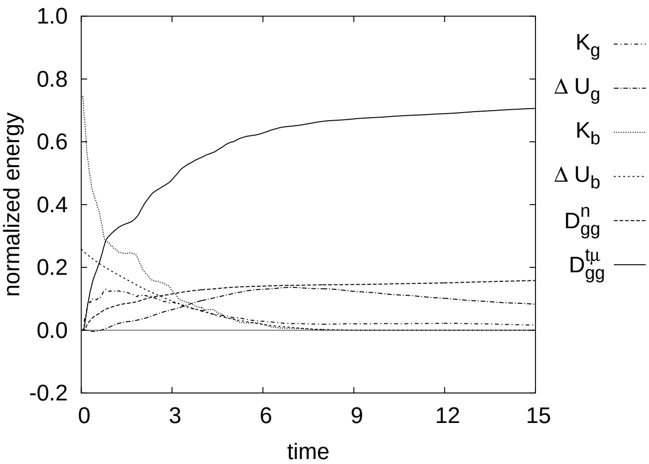

Figure 2: Different components of the ball energy and energy dissipation during impact cratering. Parameters are the same as in Fig.1

during impact which include (i) lifting of grains during crater formation; (ii) inelastic collisions between the body and the grains and among the grains during impact; (iii) friction due to particle-particle sliding contacts and body-grain sliding.

Figure 2 demonstrates the components of energy and the dissipation of energy during the impact cratering for one of the typical runs. As seen from this Figure, in the beginning roughly 25% of energy is in the form of potential energy ΔU_b and 75% is kinetic energy K_b. Most of the stored mechanical energy of the ball is transformed into the kinetic energy of the grains K_g, however its share remains relatively small (reaches ∼10% in the initial phase of impact and then slowly decays to zero) since it is immediately lost due to inelastic collisions (D^n_{gg}), friction ($D^{t\mu}_{gg}$), and change in the gravitational grain energy (ΔU_g). It follows from our simulations that most of the ball energy eventually is dissipated through the frictional contacts among the grains (about 70%), about 20% is lost due to inelastric collisions, and about 10% is spent on the change in the gravitational energy of the grains. The energy losses on friction between the ball and the grains are negligible.

3 PENETRATION DEPTH SCALING

3.1 *Previous work*

Let us summarize the recently obtained laboratory data for the penetration depth scaling with impact velocity, ball size and density. For small impact speeds, Durian with coworkers (Uehara et al. 2003) found the following scaling relationship between the crater depth d (defined as the distance between the unperturbed surface and the lowest point of the projectile at rest) and other parameters of the impact

$$d = 0.14\mu^{-1}(\rho_b/\rho_g)^{1/2}D_b^{2/3}H^{1/3} \qquad (1)$$

Here ρ_g, ρ_b are densities of grains and the ball, respectively, μ is the grain-grain friction coefficient defined through the repose angle of the grains θ, $\mu = tan\theta$, D_b is the diameter of the ball, and H is the total drop of the ball (the sum of the free-fall height $h = v_0^2/2g$ and the total penetration depth d). Equation (1) implies that there is a minimum penetration depth

$$d_0 = (0.14/\mu)^{3/2}(\rho_b/\rho_g)^{3/4}D_b \qquad (2)$$

which corresponds to the zero initial velocity impact.

On the other hand, Swinney and co-workers (Ciamarra et al. 2004) found that after a relatively short initial phase, a "penetration phase" ensues during which the deceleration of the ball a is roughly constant, which is consistent with the classical Robins-Euler model of impact (Robins 1742; Euler 1745). This scaling implies that the stopping time is independent of the initial velocity, and the penetration depth is proportional to the square of initial velocity,

$$d = v_0^2/2a. \qquad (3)$$

Finally, de Bruyn with coworkers (Walsh et al. 2003) reported a linear scaling between the ball penetration depth and the impact momentum mv_0.

The established theory of impact penetration (see, e.g. (Forrestal & Luk. 1992; Allen, Mayfield, & Morrison 1957)) is based on the so-called Poncelet model which assumes that the force acting on the object consists of three components: gravity $m_b g$, static resistance force F_s, and dynamics frictional force αv^2. The Newton law is then written as

$$m_b\ddot{s} = m_b g - F_s - \alpha\dot{s}^2 \qquad (4)$$

where $s(t)$ is the vertical coordinate of the lowest tip of the object with respect to the unperturbed free surface (see Figure 1,c,d). Integrating this equation with conditions $s(0) = 0, \dot{s}(0) = v_0, s(t_m) = d, \dot{s}(t_m) = 0$ assuming constant F_s and α yields the Poncelet formula for the maximum penetration depth

$$d = (2\alpha)^{-1}\log[1 + \alpha v_0^2(F_s - m_b g)^{-1}] \qquad (5)$$

The dimensional parameter α is proportional to the crossection of the projectile. This formula works reasonably well for medium- and high-speed impacts, however it fails to describe low-speed craters. In particular, it predicts zero penetration for zero initial velocity impact: for $v_0 = 0$, $d_0 = 0$ while in fact (especially, for loose grains) a heavy ball released at the surface produces a shallow crater by its weight. Notice that formula (5) is rather different from both (1) and (3).

3.2 *Generalized Poncelet model*

Here we attempt to generalize (4) (and correspondingly Eq.(5)) in order to describe low-speed impacts. The most important effect that needs to be taken into account is the depth-dependence of the static resistance force.

Albert et al. (Albert et al. 1998) showed experimentally that in a slow drag regime the force acting on an object is proportional to its crossection times the local pressure (or, in case of pressure varying across the object, the overall force can be obtained by integration of the pressure over the crossection). Along similar lines, one can calculate the quasi-static resistance force for the penetrating body. Figure 1c,d shows schematically the initial phase and penetration phase of the impact. In the initial phase the free surface can be considered fixed at $s = 0$, and the pressure can be taken as $p = \rho_g g s$ (here ρ_g is the effective density of the granular material). In the penetration phase, the free surface moves down with the ball, so the pressure under the ball can be taken in the form $p = \rho_g g s_0$. Here $s_0 = s - s_{\rm sf} = const = O(D_b)$ and $s_{\rm sf}$ is the free surface location near the ball. Performing calculations in 3D we obtain the static drag force

$$F_s = \begin{cases} \eta\rho_g g s^2 D_b, & s \ll D_b \\ \eta\rho_g g s_0^2 D_b, & s \gg D_b \end{cases} \tag{6}$$

and in 2D

$$F_s = \begin{cases} \eta\rho_g g s^{3/2} D_b^{1/2}, & s \ll D_b \\ \eta\rho_g g s_0^{3/2} D_b^{1/2}, & s \gg D_b \end{cases} \tag{7}$$

where η is a non-dimensional parameter dependent on the material properties of the grain and the ball (e.g., friction coefficients).

Using formulas (6),(7), we can evaluate the penetration depth as a function of initial velocity v_0. It is especially simple in case of small v_0 when one can neglect $\alpha\dot{s}^2$ in Eq.(4). Then we get $v_0^2/2 = -gd + \int_0^d F_s(s)ds/m_b$. For 3D case we get

$$4\pi^2\rho_b(3\eta\rho_g)^{-1} H D_b^2 = \begin{cases} d^3/3, & d \ll D_p \\ s_0^2 d & d \gg D_p \end{cases}, \tag{8}$$

and for 2D case we get

$$\pi\rho_b(\eta\rho_g)^{-1} H D_b^{3/2} = \begin{cases} 2d^{5/2}/5, & d \ll D_p \\ s_0^{3/2} d, & d \gg D_p \end{cases} \tag{9}$$

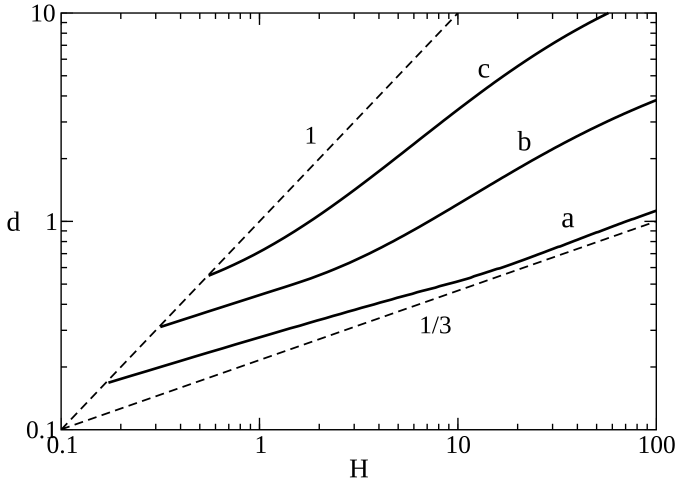

Figure 3: The final penetration depth as a function of the initial ball energy H according to the model (10) with $A = 100,\ B = 1$ for three values of $\rho_g/\rho_b = 1(a),\ 0.3(b), 0.1(c)$. Two dashed lines indicate scalings $d \propto H$ and $d \propto H^{1/3}$.

where $H = d + v_0^2/2g$. As one can see, for small impact energies, the 3D scaling agrees with the experimental results of the Durian's group, and for larger impact energy the model describes the transition to the "penetration phase" with constant deceleration in agreement with Ciamarra et al. (Ciamarra et al. 2004). The zero-initial-velocity scaling is recovered by taking $H = d$, then we get $d \propto D_b$ both in 2d and 3d cases in agreement with (1). In the intermediate range of depths $d \sim D_b$ there is no simple power-law scaling between the energy and the penetration depth. However, for large impact energies, the omitted kinetic friction term $\alpha\dot{s}^2$ has to be taken into account, which affects the initial phase of the object deceleration. Interestingly, the additional deceleration caused by the kinetic friction reduces the depth of penetration such that it deviates from the linear scaling even for large penetration depths.

To analyze the penetration dynamics in the full range of initial energies, we substitute formulas (6),(7) in Eq.(4) and cast the resulting equation in the following non-dimensional form

$$\ddot{x} = 1 - \rho_g\rho_b^{-1}(Af(x) + B\dot{x}^2) \tag{10}$$

where $x = s/D_b$, $f(x) = F_s(D_b x)/m_b g$, and A and B are non-dimensional constants. For simplicity we assume that the function $f(x)$ has a piecewise form matching the two asymptotic regimes in (6) or (7) in the point $x = 1/2$. Figure 3 shows the dependence of the penetration depth on the total impact energy according to Eq.(10) for the 3D case (when $f(x) = x^2$ at $x < 1/2$ and 1/4 otherwise).

3.3 *Scaling of our penetration data*

We performed a series of 2d simulations with different material parameters of the ball and the grains (density, friction coefficient, ball size and initial velocity) in order to verify the scaling of the penetra-

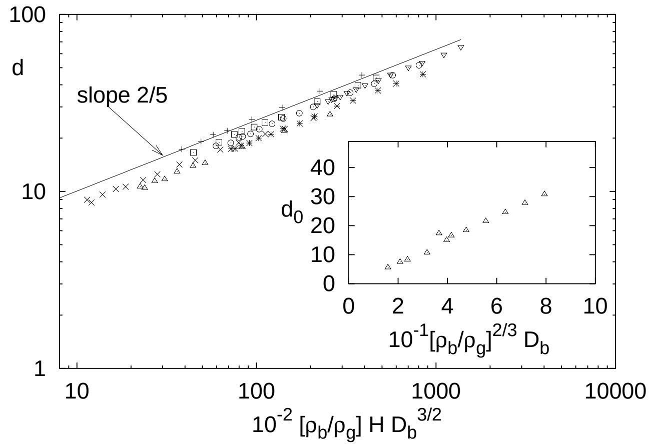

Figure 4: Scaling of the final penetration depth data with non-dimensional impact energy for different runs corresponding to different sizes and densities of the ball: $\triangle,\ D_b = 30, \rho_b/\rho_g = 1$, $\nabla,\ D_b = 50, \rho_b/\rho_g = 2$, $\circ,\ D_b = 30, \rho_b/\rho_g = 2$, $\Box,\ D_b = 20, \rho_b/\rho_g = 3$, $*,\ D_b = 50, \rho_b/\rho_g = 1$, $\times,\ D_b = 10, \rho_b/\rho_g = 3$, $+,\ D_b = 10, \rho_b/\rho_g = 7$. Inset: final penetration depth for different ball sizes and densities corresponding to zero initial velocity

tion depth with initial mechanical energy (9). Figure 4 shows the data from different runs collapsed on a single plot using the scaled variables suggested in (Uehara et al. 2003). As seen from this figure, the data collapse close to a single straight line in logarithmic coordinates which corresponds to a scaling $d \propto H^{\xi}$ with ξ close to 2/5 suggested by formula (9). We also found that the depth of the crater for a ball with zero initial velocity at impact scales linearly with the ball size (see Figure 4,Inset).

These results suggest that for small initial speeds, the penetration depth scaling is reasonably well described by the Poncelet equation (4) with depth-dependent static friction force (6),(7).

This work was supported by the U.S. DOE, grant DE-FG02-04ER46135.

REFERENCES

Albert, R., Pfeifer, M., Barabási, A.-L., & Schiffer, P. 1998. Slow drag in a granular medium. *Phys. Rev. Lett. 82*(205).

Allen, W., Mayfield, E., & Morrison, H. 1957. Dynamics of a projectile penetrating sand. *J. Appl. Phys. 28*(3): 370–376.

Ciamarra, M., Lara, A., Lee, A., Goldman, D., Vishik, I., & Swinney, H. 2004. Dynamics of drag and force distributions for projectile impact in a granular medium. *Phys. Rev. Lett. 92*(194301).

Cundall, P. A. & Strack, O. D. L. 1979. A discrete numerical model for granular assemblies. *Géotechnique* 29.

de Bruyn, J. & Walsh, A. 2004. Penetration of spheres into loose granular media. *Can. J. Phys.* 82: 439–446.

Euler, L. 1745. *Neue Grundsätze der Artillerie;* reprinted in *Euler's Opera Omnia*. Druck und Verlag Von B.G. Teubner, Berlin, 1922.

Forrestal, M. & Luk., V. 1992. Penetration into soil targets. *Int. J. Impact Eng. 12*(3): 427–444.

Newhall, K. & Durian, D. 2003. Projectile-shape dependence of impact craters in loose granular media. *Phys. Rev. E 68*(060301).

Poncelet, J. V. 1829. *Cours de Mécanique Industrielle*. Paris.

Robins, B. 1742. *New Priniples of Gunnery*. London.

Schäfer, J., Dippel, S., & Wolf, D. 1996. Force schemes in simulations of granular materials. *J. Phys. I France* 6: 5–20.

Uehara, J., Ambroso, M., Ojha, R., & Durian, D. 2003. Low-speed impact craters in loose granular media. *Phys. Rev. Lett. 90*(194301).

Volfson, D., L.S.Tsimring, & I.S.Aranson 2003. Partially fluidized shear granular flows: MD simulations and continuum theory. *Phys. Rev. E 68*(021301).

Walsh, A., Holloway, K., Habdas, P., & de Bruyn, J. 2003. Morphology and scaling of impact craters in granular media. *Phys. Rev. Lett. 91*(104301).